



# HHS Public Access

Author manuscript

*Nat Chem Biol.* Author manuscript; available in PMC 2011 March 08.

Published in final edited form as:

*Nat Chem Biol.* 2010 May ; 6(5): 352–358. doi:10.1038/nchembio.347.

## The role of conformational entropy in molecular recognition by calmodulin

Michael S. Marlow\*, Jakob Dogan\*, Kendra K. Frederick, Kathleen G. Valentine, and A. Joshua Wand

Johnson Research Foundation and Department of Biochemistry & Biophysics, University of Pennsylvania, Philadelphia, Pennsylvania 19104-6059

### Abstract

The physical basis for high affinity interactions involving proteins is complex and potentially involves a range of energetic contributions. Among these are changes in protein conformational entropy, which cannot yet be reliably computed from molecular structures. We have recently employed changes in conformational dynamics as a proxy for changes in conformational entropy of calmodulin upon association with domains from regulated proteins. The apparent change in conformational entropy was linearly related to the overall binding entropy. This view warrants a more quantitative foundation. Here we calibrate an “entropy meter” employing an experimental dynamical proxy based on NMR relaxation and show that changes in the conformational entropy of calmodulin are a significant component of the energetics of binding. Furthermore, the distribution of motion at the interface between the target domain and calmodulin are surprisingly non-complementary. These observations promote modification of our understanding of the energetics of protein-ligand interactions.

---

The formation of protein complexes involves a complicated manifold of interactions that often includes dozens of amino acids and thousands of square Ångstroms of contact area<sup>1</sup>. The origins of high affinity interactions are quite diverse and complex<sup>2</sup> and are reflected in the difficulty of computing the energetics of interactions between proteins using molecular structure alone<sup>2</sup>. Indeed, structure-based design of pharmaceuticals has been impeded by this barrier<sup>3</sup>. Of interest here is the role of protein conformational entropy in modulating the free energy of the association of a protein with a ligand. Decomposition of the total binding free energy emphasizes that the entropy of binding is comprised of contributions from the protein, the ligand and the solvent:

---

Users may view, print, copy, download and text and data- mine the content in such documents, for the purposes of academic research, subject always to the full Conditions of use: [http://www.nature.com/authors/editorial\\_policies/license.html#terms](http://www.nature.com/authors/editorial_policies/license.html#terms)

Contact Information: Professor A. Joshua Wand 905 Stellar Chance Laboratories Department of Biochemistry & Biophysics University of Pennsylvania School of Medicine 422 Curie Blvd. Philadelphia, PA 19104-6059 telephone: 215-573-7288 facsimile: 215-573-7290 wand@mail.med.upenn.edu.

\*These authors contributed equally

AUTHOR CONTRIBUTIONS A.J.W. devised and initiated the project. M.S.M., J.D., K.G.V. and K.K.F. prepared the materials, collected and analyzed the primary data. M.S.M, J.D. and A.J.W. performed the analysis. A.J.W. wrote the manuscript.

The authors declare that they have no competing financial interests.

Note supplementary information is available on the Nature Chemical Biology website.

COMPETING FINANCIAL INTERESTS The authors declare no competing financial interests.

$$\Delta G_{tot} = \Delta H_{tot} - T \Delta S_{tot} = \Delta H_{bind} - T (\Delta S_{protein} + \Delta S_{ligand} + \Delta S_{solvent}) \quad (1)$$

Historically, the contributions by solvent entropy have taken center stage and are usually framed in terms of the so-called hydrophobic effect<sup>4</sup>. Hydrophobic solvation by water continues to be the subject of extensive analysis<sup>5,6</sup>. In principle, the entropic contributions of a structured protein to the binding of a ligand ( $S_{protein}$ ) includes both changes in its internal conformational entropy ( $S_{conf}$ ) as well as changes in rotational and translational entropy ( $S_{RT}$ )<sup>7</sup>. Equation 1 emphasizes that the measurement of the entropy of binding does not resolve contributions from internal protein conformational entropy. Despite the suggestion that the conformational entropy of structured proteins is significant<sup>8,9</sup>, it is only recently that experimental evidence has become available to indicate that it is sufficiently responsive to influence the thermodynamics of protein association<sup>10,11</sup>.

Experimental measurement of  $S_{conf}$  has been difficult. Motion between different microscopic structural states has been developed as an indirect measure of or proxy for conformational entropy<sup>12</sup>. Motion expressed on the sub-nanosecond timescale corresponds to significant entropy<sup>13</sup> and NMR relaxation methods are particularly well suited for its characterization<sup>12</sup>. Previously we employed calmodulin as a model system to investigate the role of conformational entropy in the high affinity association of proteins<sup>11</sup>. Calmodulin is central to calcium-mediated signal transduction pathways of eukaryotes<sup>14</sup> and interacts with hundreds of proteins with high affinity<sup>15</sup>. Using NMR relaxation methods, we have shown that calcium-saturated calmodulin (CaM) is an unusually dynamic protein and is characterized by a broad distribution of the amplitudes of fast side-chain dynamics<sup>10</sup>. The binding of target domains causes a redistribution of these motions in calmodulin<sup>10,11</sup>. Interpretation of the changes in motion using a simple harmonic oscillator model<sup>13</sup> yielded a remarkable linear correlation between the apparent change in conformational entropy of CaM and the total binding entropy<sup>11</sup>. Taken at face value, this suggested a considerable contribution from conformational entropy to the total binding entropy and indicated a role for conformational entropy in “tuning” calmodulin’s high affinity interactions.

However, the analytical strategy employed suffers from several potential limitations<sup>11,12</sup>. That approach effectively takes an inventory of the change in motion at a limited number of sites and interprets this within the context of a simple physical model such as the harmonic oscillator<sup>13</sup>. This raises several issues including the effects of correlated motion, the operation of a more complex potential energy function, the completeness of the oscillator count, and so on<sup>12</sup>. Although the presence of a linear correlation between the apparent change in conformational entropy and total binding entropy is a compelling indication of the importance of the former, the quantitative scale of the interpreted  $S_{conf}$  is potentially suspect. Here we resolve this issue by taking a different approach based on an empirical calibration of the dynamical proxy for conformational entropy. Rather than attempt a model-dependent interpretation of an inventory of changes in local dynamics, we use experimental measures of local dynamics as a proxy for local disorder and seek an empirical scaling between them. The aim is to effectively solve for each term of equation (1). An essential component of this approach is knowledge of the dynamics of the target domains, which are determined here. The availability of these data allows for the quantitative calibration of the

dynamical proxy for conformational entropy. It is revealed that the conformational entropy of calmodulin not only contributes significantly to the free energy of binding of target domains but also appears to be the dominant factor in tuning the affinity of calmodulin for the various target domains examined.

## RESULTS

### Dynamics of the target domains in complex with CaM

Using deuterium NMR relaxation methods<sup>16</sup>, we examined fast motion of the methyl-bearing side-chains of the target domains in the six CaM complexes examined previously<sup>11</sup>. These include complexes between calmodulin and the calmodulin-binding domains of the endothelial and neuronal nitric oxide synthases (eNOS and nNOS, respectively), calmodulin kinase kinase alpha (CaMKK $\alpha$ ), calmodulin kinase I (CaMKI), phosphodiesterase (PDE) and the smooth muscle myosin light chain kinase (smMLCK). The calmodulin-binding domains are represented here as peptides and we will use the nomenclature eNOS(p), for example, to emphasize this fact. All peptide domains have a basic amphiphilic sequences, typical of CaM binding domains (Supplementary Table 1). These domains have been found by isothermal titration calorimetry at 308 K to bind with roughly the same affinity to CaM but with widely different thermodynamic parameters defining the free energy of association<sup>11, 17, 18</sup>. In the case of the CaMKK $\alpha$ (p) and smMLCK(p) domains, binding is driven by a large favorable change in total binding enthalpy overcoming a large unfavorable change in total binding entropy. At the other extreme, nNOS(p) binding is driven by a favorable change in total enthalpy accompanied by a small favorable change in entropy. The other domains represent intermediate cases. The entropy of binding of these domains varies by 90 kJ/mole and changes sign (Supplementary Table 2)<sup>11</sup>.

All bound target domain methyl resonances are well resolved in <sup>13</sup>C- NMR spectra and deuterium relaxation parameters could be measured with high precision (Supplementary Fig. 1). The degree of spatial restriction of each motional probe was assigned a number between 0, corresponding to complete isotropic disorder, and 1, corresponding to a fixed orientation within the molecular frame. This parameter is the so-called model-free squared generalized order parameter<sup>19</sup> as it applies to the methyl symmetry axis ( $O^2_{axis}$ ). A recent re-evaluation of the model-free treatment of Lipari & Szabo reinforces confidence in its robustness with respect to highly asymmetric side chain motion<sup>20</sup>. The 80 methyl  $O^2_{axis}$  parameters from 53 residues of the target domains in the six wild-type CaM complexes are heterogeneously distributed with  $O^2_{axis}$  values ranging from 0.05 to 0.95 (Fig. 1). The distribution is non-uniform and reminiscent of the multi-modal distributions of the calmodulin component of these complexes<sup>11</sup>.

### Variable and counter-intuitive motion at the interface

The methyl bearing side-chains of the target domains are distributed throughout the CaM-peptide interface providing an excellent system to examine the intricacies of structure-dynamics relationships. The structures of all but the complex with PDE(p) are known. CaM-target complexes have “anchor” residues that localize to hydrophobic pockets formed by the amino and carboxy-terminal domains of CaM. Typically, one anchor residue is aromatic

(Trp or Phe) and the other aliphatic. Anchor residues are believed to be essential for complex formation<sup>21</sup>. The aliphatic side-chain anchors of the bound target domains are localized to the amino-terminal domain of CaM (Fig. 2). Surprisingly, most aliphatic peptide side chains historically identified as “anchor” residues are more dynamic than one might expect. Specifically, the  $O^2_{axis}$  values of eNOS(p) and nNOS(p) leucine  $\delta$  methyls and the CaMKI(p) methionine  $\epsilon$  methyl are at or below the residue-specific averages for the CaM complexes (Supplementary Table 3). With L19 of smMLCK(p) providing the lone exception, the binding within the pocket need not significantly confine the motion of the anchor residues of the bound target domain.

Complex formation results in a striking pattern of the dynamics of the CaM methyl-bearing residues that form the binding pocket (I27, L32, M51, I52, V55, I63, and M71). For example, in every complex I27 $\delta$  and I63 $\delta$  exhibit relatively restricted motion with an average  $O^2_{axis}$  of 0.69 ( $n = 12$ ), which is 0.19 greater than the residue average for isoleucine  $\delta$ -methyls in the CaM complexes. In contrast, the  $O^2_{axis}$  for the  $\delta$ -methyl of I52 averages 0.36 ( $n = 6$ ), which is 0.14 less than the residue average in the CaM complexes. The average  $O^2_{axis}$  for the  $\delta$ -methyls of L32 of 0.50 ( $n = 12$ ) is also significantly smaller than the residue average of 0.60. A similar pattern is seen in the residues found in the carboxy-terminal pocket that bind aromatic peptide anchor residues. Some residues, such as L105 and V136, have methyl group dynamics at their residue specific averages in the CaM complexes. Others are highly constrained such as I100 $\delta$  ( $n = 5$ ) and A128 ( $n = 5$ ), which show average  $O^2_{axis}$  that are 0.3 and 0.23 larger than the residue averages. Clearly, binding does not induce a uniform reduction in side-chain motion within the hydrophobic pockets. More nuanced responses are also seen. This may be a feature of proteins that have evolved to bind numerous targets. Such responses motivates extending the view of hot spot interactions<sup>22</sup> to include resolution of dynamical (entropic) from specific enthalpic contributions.

### Calibration of the “entropy meter”

We now turn to the insights into the thermodynamic origins of binding offered by the characterization of internal motion in the calmodulin complexes. A main goal is to empirically calibrate the dynamical proxy of conformational entropy for the calmodulin system. We first decompose the entropy of binding in terms of contributions from calmodulin, the target domains and solvent:

$$\Delta S_{tot} = \Delta S_{conf}^{CaM} + \Delta S_{conf}^{target} + \Delta S_{sol} + \Delta S_{RT} \quad (2)$$

Contributions from rotational and translational entropy of CaM and the peptide ( $S_{RT}$ ) have been grouped. The similarity in peptide lengths, the structures of the complexes, and the binding affinities suggest that  $S_{RT}$  is essentially constant across the complexes. We further postulate that the contribution of changes in the conformational entropy of CaM and the target domains are linearly related to local disorder represented by the squared generalized order parameters determined by NMR relaxation in methyl groups:

$$\Delta S_{conf} = m \left[ \left( n_{res}^{CaM} g \langle \Delta O_{axis}^2 \rangle^{CaM} + n_{res}^{target} g \langle \Delta O_{axis}^2 \rangle^{target} \right) \right] + \Delta S_{other} \quad (3)$$

The parameter  $m$  defines the scaling between average changes in residue weighted generalized order parameters for calmodulin and the target domain upon binding (i.e.  $\langle \Delta O_{axis}^2 \rangle = \langle \Delta O_{axis}^2 (\text{complexed}) \rangle - \langle \Delta O_{axis}^2 (\text{free}) \rangle$ , where  $n_{res}^{CaM}$  and  $n_{res}^{target}$  are the number of residues in CaM and a given target domain, respectively, used in the entropy calibration (See Supplementary Table 1 for further explanation). Equation (3) includes potential contributions ( $S_{other}$ ) from other sources conformational entropy of the protein that are not sensed (directly or indirectly) by the deuterium NMR relaxation probes used here. This includes, for example, vibrational entropy involving motion that does not average the angle of the methyl symmetry axis with the magnetic field and motion slower than overall tumbling of the macromolecule<sup>12</sup>. We assume that these other contributions ( $S_{other}$ ) are the same for all target peptides and complexes, which is not unreasonable given that the peptides all have roughly the same number of degrees of freedom. This leads to the prediction of a linear relationship between the difference of the total binding entropy and the solvent entropy and the apparent change in conformational entropy measured by NMR relaxation:

$$(\Delta S_{tot} - \Delta S_{sol}) = m \left[ \left( n_{res}^{CaM} g \langle \Delta O_{axis}^2 \rangle^{CaM} + n_{res}^{target} g \langle \Delta O_{axis}^2 \rangle^{target} \right) \right] + \Delta S_{RT} + \Delta S_{other} \quad (4)$$

Some of the assumptions leading to Equation (4) may appear drastic. However, should any of them be violated, a significant deviation from linearity should be observed.

As suggested by Equation (4), to compare dynamics in the various complexes we employ a normalization procedure to account for variation in the number of methyl sites in CaM whose motion could be quantified and to account for the fact that, although fully resolved, the number of residues in the target domains vary. A simple average was employed (see Equation (4) and Supplementary Table 4). The apparent change in conformational entropy due to fast motion was then calculated without explicit consideration of the classical entropy due to rotamer interconversion<sup>11,23</sup>. This entropy will be contained within the calibrated dynamical proxy (i.e., within the scalar  $m$ ). As the free target states cannot be assessed using the model-free formalism<sup>19</sup>, we assume that the dynamics of the free unstructured target domains are uniform and correspond to an  $O_{axis}^2$  of 0.05. This limiting value is seen, for example, in Val-3 of CaMKK $\alpha$ (p) bound to CaM, which is completely solvent exposed and hence provides a internal reference for unrestricted motion that meets the criteria of the model-free treatment.

The  $O_{axis}^2$  parameter only detects motion on a timescales significantly shorter than the macromolecular tumbling, which for these complexes is on the order of 8.5 ns<sup>11</sup>. States that interconvert on the  $\mu$ s-ms timescale are illuminated by chemical shift averaging effects<sup>24</sup>. Methyl dispersion experiments of the CaM:smMLCK(p) and CaM:nNOS(p) complexes indicate that these complexes are silent in this time regime. States that are not averaged on the chemical shift times scale are indicated by the presence of minor components in the NMR spectrum. A small amount of micro-heterogeneity was observed in CaM in some of the complexes<sup>11</sup>. This is a small contribution that we ignore. There is no micro-heterogeneity of side-chain conformations of the bound target domains evident in their <sup>13</sup>C-

HSQC spectra and the corresponding contribution to the conformational entropy was taken to be zero.

To solve equation (4), we use the binding entropies obtained by isothermal titration calorimetry<sup>11</sup> and calculate the change in solvent entropy using the known structures of free CaM<sup>25</sup> and the five complexes for which high resolution structures are available<sup>26,29</sup>. The empirical relationship between changes in accessible surface area and the entropy of solvent<sup>30</sup> is employed and calculated assuming a fully solvated structure for the dissociated target domains (see Methods and Supplementary Table 5). Not included are changes in solvent entropy due to electrostriction of water by solvation of explicit charge (however, see below). To further test this approach, we also examined the complex of a mutant CaM with the smMLCKp domain. Of several examined previously, we chose to examine the CaM(E84K):smMLCK(p) complex as it showed the most varied dynamical response compared to the wild-type complex<sup>31</sup>. The entropy of binding was determined by isothermal titration calorimetry to be  $+41 \pm 1$  kJ/mole at 308 K, which is significantly less unfavorable than the wild-type complex. The binding free energy and enthalpy were also determined to be  $-43.6 \pm 0.5$  and  $-84.3 \pm 0.8$  kJ/mole, respectively. The methyl  $O^2_{axis}$  parameters were previously determined for the complex<sup>31</sup>. To use this complex for calibration required measurement of the dynamics of the bound smMLCK(p) domain and characterization of the dynamics of the free CaM(E84K) mutant.

Equation (4) *requires* a quantitative linear relationship and is plotted for the six complexes (Fig. 3). Five given an excellent linear relationship ( $R = 0.95$ ) and a slope of  $-0.037 \pm 0.007$  kJ K<sup>-1</sup> mol<sup>-1</sup> res<sup>-1</sup> and an ordinate intercept of  $0.26 \pm 0.18$  K kJ<sup>-1</sup> mol<sup>-1</sup> res<sup>-1</sup> (Fig. 3). The CaMKKα(p) complex is a clear outlier (Fig. 3). This is not surprising. The primary sequence is unusually hydrophobic (Supplementary Table 1) and the peptide has limited solubility<sup>17</sup>. Hydrophobic cluster analysis<sup>32</sup> illuminates a hydrophobic patch and suggests that the dissociated domain exists in a collapsed, less hydrated state than is assumed for the solvent entropy calculations. A simple correction based on the size of the predicted hydrophobic cluster shows that this is not an unreasonable explanation for the apparent discrepancy (Fig. 3).

Excluding the CaMKKα(p) complex, the quantitative linearity of the remaining points strongly suggests that the assumptions underlying Equation (4) are largely valid and that a self-consistent view of the origin of the thermodynamics of binding in the calmodulin system has been established. Most important is the apparent validity of employing measures of motion as a quantitative proxy for conformational entropy. Furthermore, the quantitative consistency also suggests that the contribution of vibrational entropy, which is largely contained in the constant intercept in Fig. 3, is not *variable* across the calmodulin complexes. In this respect, it is interesting to note that the corresponding ordinate intercept is nominally positive even though the loss of rotational and translational entropy would result in a negative contribution to the ordinate intercept (see Equation 2). This apparent discrepancy is easily explained by recognizing that the formation of each of the complexes results in the burial of 6 charged side-chains through the formation of ion pairs. The removal of charge from bulk water will result in a significant increase in solvent entropy<sup>33</sup>. The degree of electrostriction in the free state can be estimated from the pressure



dependence of the formation of the CaM:smMLCK(p) complex, which has been measured using hydrogen exchange based methods<sup>34</sup>. Comparison to solvent entropy values for model charged species<sup>33</sup> suggests that this effect is comparable to the predicted positive contribution to the free energy of binding by  $S_{RT}$ . Furthermore, vibrational entropy has also been suggested to provide a favorable contribution to the binding of ligands to proteins in some cases, dihydrofolate reductase being one such example<sup>35</sup>. It is possible that an increase in vibrational entropy upon formation of the calmodulin complexes also diminishes the counter-balances the contribution of the loss of rotational and translational entropy to the ordinate intercept of Figure 3. Regardless, the linear regression statistics indicates that these contributions are constant across the five well-behaved complexes.

The possible exception of the CaM:CaMKK $\alpha$ (p) complex to the linear relationship defined by the other five complexes (Fig. 3) has several interesting implications. As noted above, this domain is expected to form a collapsed hydrophobic cluster in the free state. A simple calculation suggests that such a dehydrated cluster could significantly reduce the apparent discrepancy (see Supplementary Table 5 and Fig. 3). The resulting chain compaction would cause an opposing correction but in this situation is predicted to be relatively small<sup>36</sup>. It should be noted that the isothermal titration calorimetry profile of the formation of this complex is simple and unremarkable and does not indicate the presence of a more complex equilibrium involving the disassembly of aggregates of the target, for example<sup>17</sup>. In addition, calmodulin interacts with this domain in reverse orientation from the others, which may be reflected in the apparently anomalously higher motion of the bound domain. Despite these uncertainties about the nature of the solvent and free target domain contributions to the binding entropy of the formation of this complex, the contribution of CaM to the binding of the CaMKK $\alpha$ (p) target is consistent with the other complexes, as we will now show below.

### Insights into the role of protein entropy in binding

The dynamical proxy relating local measures of disorder quantified by the squared generalized order parameters of the symmetry axis of methyl groups to residual conformational entropy has been calibrated (Fig. 3). This allows the contributions by changes in conformational entropy to the total binding entropy to be determined (Fig. 4). The empirical calibration of measures of motion as a proxy for conformational entropy circumvents the microscopic details that are difficult to accommodate in a model-dependent calculation. In a sense, we have simply created an “entropy meter” analogous to a simple thermometer. It is important to note that in this view the motion of the methyl group is used to sense the disorder of its local surroundings.

The apparent relationship between the change in the conformational entropy of CaM and the target domains and the total entropy of binding can now be quantitatively revealed. The changes in conformational entropy of the target domains and CaM are large relative to the free energy of binding and are the same magnitude as the solvent entropy (Fig. 4 and Supplementary Table 6). Though the folding of a disordered sequence into a bound helix would result in a significant loss of conformational entropy the large opposing entropic contribution to binding by stable folded state of calmodulin is remarkable.

## DISCUSSION

The use of a dynamical proxy as an empirical “entropy meter” is more simple and precise than the “oscillator inventory” attempted previously<sup>11</sup>. It would appear that, though providing a qualitatively correct view, the “inventory” approach has significantly underestimated the contribution of conformational entropy to the binding free energy. This is perhaps not surprising. An inventory requires completeness in the sampling of motion whereas the method developed here has a quite a different view and uses local measures of motion as an indirect measure of local disorder. The latter approach does require good sampling of the volume of the protein, which is met here by the ~90 methyl groups in each of the calmodulin complexes. It also requires significant coupling of the motion of methyl groups to surrounding non-methyl amino acid side chains. The heterogeneous side chain dynamics seen generally in proteins and the similarly heterogeneous response to ligand binding seen here raises the possibility of how faithful the coupling is. Indeed, as exemplified by the variable behavior of the CaM:target domain interface (Fig. 2) the coupling at specific sites may seem distressingly variable. However, the approach illustrated here relies on the average response of dozens of probes. Indeed, as the mutant CaM complex perhaps demonstrates best, the empirical correlation of motion with conformational entropy appears to be surprisingly robust (Fig. 3).

This robustness presumably arises from several sources. The empirical calibration of the “entropy meter” developed here assumes that existence of a linear relationship between motion (i.e.  $O_{\text{axis}}^2$ ) and the local conformational entropy (disorder) sampled by the NMR spin probe. In a packed protein, this local disorder reflects not only the spin probe itself but also that of its neighbors. In addition, a wide range of potential energy functions, including the highly asymmetric step-function, show a roughly linear correlation with the corresponding  $O_{\text{axis}}^2$  parameter<sup>23</sup>. The  $O_{\text{axis}}^2$  parameters of various CaM complexes have a striking tri-modal distribution<sup>11</sup>. We have termed these groupings or classes the J-,  $\alpha$ - and  $\omega$ -classes, in accordance with the character of the motions underlying them<sup>12</sup>. The lowest  $O_{\text{axis}}^2$  parameter J-class is accompanied by rotamer interconversion<sup>23</sup> that is reflected by averaging of associated J-coupling constants. In principle this distortion of the  $O_{\text{axis}}^2$  parameter could introduce a non-linear response. However, for energetic parameters consistent with rotamer populations in packed proteins, the correlation remains largely linear<sup>23</sup>. Furthermore, the dynamical response of calmodulin is largely within these classes of motion thereby minimizing the introduction of qualitatively distinct motion on going from the free to bound state<sup>20</sup>. These various factors, when averaged over a large number of probes distributed across the entire molecule, would tend to produce a robustness to local exceptions to the assumptions underlying the use of a dynamical proxy for conformational entropy.

Ironically perhaps, the analysis presented here is somewhat limited by knowledge of the free state of the ligand. Calmodulin generally relieves auto-inhibition by competition for a pseudo-substrate sequence<sup>15</sup>. Molecular recognition of the target sequence involves its refolding on the surface of CaM<sup>34,37</sup> and is an example of “folding upon binding”<sup>38</sup>. Complexes involving structured proteins, where the NMR-based inventory of changes in conformational entropy can be undertaken directly in both the free and complexed states,



should prove more tractable. Nevertheless, the observations made here extend the database of site-resolved experimental measurements of fast dynamics in proteins<sup>12</sup>, which in turn provides challenging test sets for molecular dynamics simulations<sup>39-42</sup> and for structure-based predictions of local motion<sup>43</sup>. The results reported here represent the first quantitative experimental measure of the role conformational entropy in high affinity interactions involving proteins. As such they should provide a benchmark for theoretical analyses based on statistical thermodynamic or molecular dynamics approaches<sup>44</sup>.

The conformational entropy of CaM is linearly correlated with the total binding entropy. There is no physical requirement for such a statistical relationship. Its existence suggests roots in the evolution of the target calmodulin-binding domains and the need to resolve a complex optimization of structural specificity (molecular recognition) and affinity. It is interesting to note that calcium-saturated calmodulin is an unusually dynamic protein and this feature has clearly been exploited and may have been the solution arrived at by evolution. In effect, variation of the conformational entropy of calmodulin “tunes” the binding free energy. In contrast, the estimated increases in solvent entropy upon binding are large and favorable but only vary little with binding entropy (Fig. 4). Thus, although solvent entropy is a powerful favorable driving force for these binding interactions it has not been utilized in the evolutionary refinement of CaM’s affinity for target domains. Surprisingly, the change in the conformational entropy of the target domain is only weakly correlated with the binding entropy though there is an apparent trend opposing the contributions from CaM (Fig. 4). It is also interesting that the microscopic character of the interface between the CaM and the target domain is often counter-intuitive with prominent structural features that promote a “lock and key” view often having highly dynamical components. This emphasizes the advantages of decomposing the so-called free energy hotspots<sup>22</sup> into both microscopic enthalpic and entropic components.

The generality of the significance of conformational entropy within the overall free energy of protein-ligand associations remains unclear. Is it wide-spread? Does conformational entropy impact the interaction of small molecules with proteins, particularly in the context of protein-directed pharmaceuticals?<sup>45</sup> If so, then the current paradigm for rational based drug design will need to be modified. These questions are of fundamental importance and represent future challenges. The approach illustrated here would seem to provide a route into this emerging area of protein thermodynamics.

## METHODS

### Sample preparation

Target domains were isotopically labeled by expression in *E. coli*<sup>17</sup> as fusion proteins with 6His-tag-thioredoxin. Fusion proteins were cleaved with thrombin in the presence of CaM and the CaM:peptide complex was purified by gel filtration. The peptide was isolated from CaM by addition of EDTA and purified by reverse phase high-pressure liquid chromatography. Wild-type and the E84K mutant calmodulins were prepared as described previously<sup>31,46</sup> in 20 mM imidazole (pH 6.5), 100 mM KCl, 6 mM CaCl<sub>2</sub> and 0.02 % (w/v) NaN<sub>3</sub>. NMR samples were slightly under-titrated with peptide to ensure that all peptide was bound.

## NMR spectroscopy

Rotational correlation times for free wild-type CaM and its complexes were determined previously<sup>11</sup>. The rotational correlation times for the N- and C-terminal domains of free E84K CaM were found to be 9.0 and 8.2 ns, respectively, and were determined using <sup>15</sup>N  $T_1$  and  $T_2$  relaxation data collected at 500 and 600 MHz (<sup>1</sup>H) essentially as described previously<sup>17,31</sup>.  $O^2_{axis}$  parameters were determined from  $T_1$  and  $T_{1\rho}$  deuterium relaxation<sup>16</sup> measured at two magnetic fields at 35 °C. Model free parameters<sup>19</sup> were determined<sup>47</sup> using a quadrupolar coupling constant of 167 kHz. The average error of  $O^2_{axis}$  parameters across all complexes was estimated by Monte Carlo sampling to be 0.023. Methyl dispersion experiments used the pulse sequences reported elsewhere<sup>48</sup>.

## Data interpretation

A somewhat different and simpler approach than employed previously<sup>11</sup> was used to interpret of obtained order parameters as a proxy for conformational entropy. Rather than attempt an inventory of oscillators, we now simply use the obtained order parameters as an “entropy meter” or proxy. We use a weighted average of the change in generalized order parameters of the methyl group symmetry axes (see Equation 4), which have been directly measured for free CaM and complexed CaM<sup>11</sup> and target domains measured here. An  $O^2_{axis}$  parameter of 0.05 was used to represent the dynamics in the free target domain.

Accessible surface area was calculated using AREAIMOL from the CCP4 suite of programs<sup>49</sup>. Accessible surface area calculations were based on the structure of free CaM<sup>25</sup> and those of the five complexes using CaM residues common to all structures (Thr5-Thr146)<sup>26,29</sup> as described more fully in Supplementary Table 5. Sequence analysis<sup>32</sup> indicates the central hydrophobic residues of CaMKK $\alpha$ (p) likely form a hydrophobic cluster when free in solution (Supplementary Fig. 2). The effects of solvent exclusion on solvent entropy in the text were calculated as described in Supplementary Tables 4 and 6. Statistical tests were calculated using JMP 8.0.1 (SAS) and KaleidaGraph 4.0 (Synergy). A listing of the  $O^2_{axis}$  parameters is provided in Supplementary Table 7.

## Supplementary Material

Refer to Web version on PubMed Central for supplementary material.

## ACKNOWLEDGMENTS

We are grateful to Dr. Sabrina Bédard and Adam Seitz for preparation of materials. We thank Professor Kim Sharp for helpful discussion and Drs. James K. Kranz and David Hokansen for preparation of some materials used in preliminary experiments. This work was supported by a grant from the National Institutes of Health (DK 39806). K.K.F. was an NIH pre-doctoral trainee (GM 08275). J.D. acknowledges financial support from the Wenner-Gren Foundations.

## References

1. Wodak SJ, Janin J. Structural basis of macromolecular recognition. *Adv. Prot. Chem.* 2002; 61:9–73.

2. Gilson MK, Given JA, Bush BL, McCammon JA. The statistical-thermodynamic basis for computation of binding affinities: a critical review. *Biophys. J.* 1997; 72:1047–69. [PubMed: 9138555]
3. Homans SW. Water, water everywhere - except where it matters? *Drug Disc. Today.* 2007; 12:534–9.
4. Tanford C. The hydrophobic effect and the organization of living matter. *Science.* 1978; 200:1012–8. [PubMed: 653353]
5. Sharp KA, Nicholls A, Fine RF, Honig B. Reconciling the magnitude of the microscopic and macroscopic hydrophobic effects. *Science.* 1991; 252:106–9. [PubMed: 2011744]
6. Chandler D. Interfaces and the driving force of hydrophobic assembly. *Nature.* 2005; 437:640–7. [PubMed: 16193038]
7. Steinberg IZ, Scheraga HA. Entropy changes accompanying association reactions of proteins. *J. Biol. Chem.* 1963; 238:172–81. [PubMed: 13983721]
8. Karplus M, Ichiye T, Pettitt BM. Configurational entropy of native proteins. *Biophys. J.* 1987; 52:1083–5. [PubMed: 3427197]
9. Matthews BW. Genetic and structural analysis of the proteins stability problem. *Biochemistry.* 1987; 26:6885–6888. [PubMed: 3427049]
10. Lee AL, Kinnear SA, Wand AJ. Redistribution and loss of side chain entropy upon formation of a calmodulin-peptide complex. *Nat. Struct. Biol.* 2000; 7:72–77. [PubMed: 10625431]
11. Frederick KK, Marlow MS, Valentine KG, Wand AJ. Conformational entropy in molecular recognition by proteins. *Nature.* 2007; 448:325–9. [PubMed: 17637663]
12. Igumenova TI, Frederick KK, Wand AJ. Characterization of the fast dynamics of protein amino acid side chains using NMR relaxation in solution. *Chem. Rev.* 2006; 106:1672–99. [PubMed: 16683749]
13. Li Z, Raychaudhuri S, Wand AJ. Insights into the local residual entropy of proteins provided by NMR relaxation. *Prot. Sci.* 1996; 5:2647–50.
14. Kahl CR, Means AR. Regulation of cell cycle progression by calcium/calmodulin-dependent pathways. *Endocr. Rev.* 2003; 24:719–36. [PubMed: 14671000]
15. Yap KL, et al. Calmodulin target database. *J. Struct. Funct. Genom.* 2000; 1:8–14.
16. Muhandiram DR, Yamazaki T, Sykes BD, Kay LE. Measurement of H-2 T-1 and T-1 $\rho$  relaxation-times in uniformly C-13-Labeled and fractionally H-2-labeled proteins in solution. *J. Am. Chem. Soc.* 1995; 117:11536–11544.
17. Marlow MS, Wand AJ. Conformational dynamics of calmodulin in complex with the calmodulin-dependent kinase kinase alpha calmodulin-binding domain. *Biochemistry.* 2006; 45:8732–41. [PubMed: 16846216]
18. Frederick KK, Kranz JK, Wand AJ. Characterization of the backbone and side chain dynamics of the CaM-CaMKII $\alpha$  complex reveals microscopic contributions to protein conformational entropy. *Biochemistry.* 2006; 45:9841–8. [PubMed: 16893184]
19. Lipari G, Szabo A. Model-free approach to the interpretation of nuclear magnetic resonance relaxation in macromolecules. 1. Theory and range of validity. *J. Am. Chem. Soc.* 1982; 104:4546–4559.
20. Frederick KK, Sharp KA, Warischalk N, Wand AJ. Re-evaluation of the model-free analysis of fast internal motion in proteins using NMR relaxation. *J. Phys. Chem. B.* 2008; 112:2095–12103. [PubMed: 18229915]
21. Crivici A, Ikura M. Molecular and structural basis of target recognition by calmodulin. *Annu. Rev. Biophys. Biomol. Struct.* 1995; 24:85–116. [PubMed: 7663132]
22. Clackson T, Wells JA. A hot spot of binding energy in a hormone-receptor interface. *Science.* 1995; 267:383–6. [PubMed: 7529940]
23. Lee AL, Sharp KA, Kranz JK, Song XJ, Wand AJ. Temperature dependence of the internal dynamics of a calmodulin-peptide complex. *Biochemistry.* 2002; 41:13814–13825. [PubMed: 12427045]

24. Palmer AGI, Massi F. Characterization of the dynamics of biomacromolecules using rotating-frame spin relaxation NMR spectroscopy. *Chem. Rev.* 2006; 106:1700–1719. [PubMed: 16683750]
25. Kainosho M, et al. Optimal isotope labelling for NMR protein structure determinations. *Nature.* 2006; 440:52–7. [PubMed: 16511487]
26. Aoyagi M, Arvai AS, Tainer JA, Getzoff ED. Structural basis for endothelial nitric oxide synthase binding to calmodulin. *EMBO J.* 2003; 22:766–75. [PubMed: 12574113]
27. Meador WE, Means AR, Quijcho FA. Target enzyme recognition by calmodulin: 2.4 Å structure of a calmodulin-peptide complex. *Science.* 1992; 257:1251–5. [PubMed: 1519061]
28. Clapperton JA, Martin SR, Smerdon SJ, Gambin SJ, Bayley PM. Structure of the complex of calmodulin with the target sequence of calmodulin-dependent protein kinase I: studies of the kinase activation mechanism. *Biochemistry.* 2002; 41:14669–79. [PubMed: 12475216]
29. Osawa M, et al. A novel target recognition revealed by calmodulin in complex with Ca<sup>2+</sup>-calmodulin-dependent kinase kinase. *Nat. Struct. Biol.* 1999; 6:819–24. [PubMed: 10467092]
30. D'Aquino JA, et al. The magnitude of the backbone conformational entropy change in protein folding. *Proteins.* 1996; 25:143–156. [PubMed: 8811731]
31. Igumenova TI, Lee AL, Wand AJ. Backbone and side chain dynamics of mutant calmodulin-peptide complexes. *Biochemistry.* 2005; 44:12627–39. [PubMed: 16171378]
32. Gaboriaud C, Bissery V, Benchetrit T, Mornon JP. Hydrophobic cluster analysis: an efficient new way to compare and analyse amino acid sequences. *FEBS Lett.* 1987; 224:149–55. [PubMed: 3678489]
33. Marcus Y. Ionic volumes in solution. *Biophys. Chem.* 2006; 124:200–7. [PubMed: 16793195]
34. Kranz JK, Flynn PF, Fuentes EJ, Wand AJ. Dissection of the pathway of molecular recognition by calmodulin. *Biochemistry.* 2002; 41:2599–608. [PubMed: 11851407]
35. Balog E, et al. Direct determination of vibrational density of states change on ligand binding to a protein. *Phys. Rev. Lett.* 2004; 93 Article Number 028103.
36. Bromberg S, Dill KA. Side-chain entropy and packing in proteins. *Prot. Sci.* 1994; 3:997–1009.
37. Ehrhardt MR, Urbauer JL, Wand AJ. The energetics and dynamics of molecular recognition by calmodulin. *Biochemistry.* 1995; 34:2731–2738. [PubMed: 7893684]
38. Dyson HJ, Wright PE. Coupling of folding and binding for unstructured proteins. *Cur. Opin. Struct. Biol.* 2005; 12:54–60.
39. Chatfield DC, Szabo A, Brooks BR. Molecular dynamics of staphylococcal nuclease: Comparison of simulation with N-15 and C-13 NMR relaxation data. *J. Am. Chem. Soc.* 1998; 120:5301–5311.
40. Prabhu NV, Lee AL, Wand AJ, Sharp KA. Dynamics and entropy of a calmodulin-peptide complex studied by NMR and molecular dynamics. *Biochemistry.* 2003; 42:562–570. [PubMed: 12525185]
41. Showalter SA, Bruschweiler R. Validation of molecular dynamics simulations of biomolecules using NMR spin relaxation as benchmarks: Application to the AMBER99SB force field. *J. Chem. Theory Comput.* 2007; 3:961–975. [PubMed: 26627416]
42. Li DW, Bruschweiler R. A dictionary for protein side-chain entropies from NMR order parameters. *J. Am. Chem. Soc.* 131:7226–7227. [PubMed: 19422234]
43. Zhang F, Bruschweiler R. Contact model for the prediction of NMR N-H order parameters in globular proteins. *J. Am. Chem. Soc.* 2008; 130:9178–9178.
44. Li DW, Bruschweiler R. In silico relationship between configurational entropy and soft degrees of freedom in proteins and peptides. *Phys. Rev. Lett.* 2009; 102 Article Number: 118108.
45. Mobley DL, Dill KA. Binding of small-molecular ligands to proteins: “What you see” is not always “What you get”. *Structure.* 2009; 17:489–498. [PubMed: 19368882]
46. Kranz JK, Lee EK, Nairn AC, Wand AJ. A direct test of the reductionist approach to structural studies of calmodulin activity: relevance of peptide models of target proteins. *J. Biol. Chem.* 2002; 277:16351–4. [PubMed: 11904288]
47. Dellwo MJ, Wand AJ. Model-independent and model-dependent analysis of the global and internal dynamics of cyclosporine-A. *J. Am. Chem. Soc.* 1989; 111:4571–4578.

48. Skrynnikov NR, Mulder FAA, Hon B, Dahlquist FW, Kay LE. Probing slow time scale dynamics at methyl-containing side chains in proteins by relaxation dispersion NMR measurements: Application to methionine residues in a cavity mutant of T4 lysozyme. *J. Am. Chem. Soc.* 2001; 123:4556–4566. [PubMed: 11457242]
49. Bailey S. The CCP4 suite - programs for protein crystallography. *Acta Cryst. D Biol. Cryst.* 1994; 50:760–763.
50. DeLano, WL. The PyMOL molecular graphics system. DeLano Scientific; San Carlos, CA: 2002.

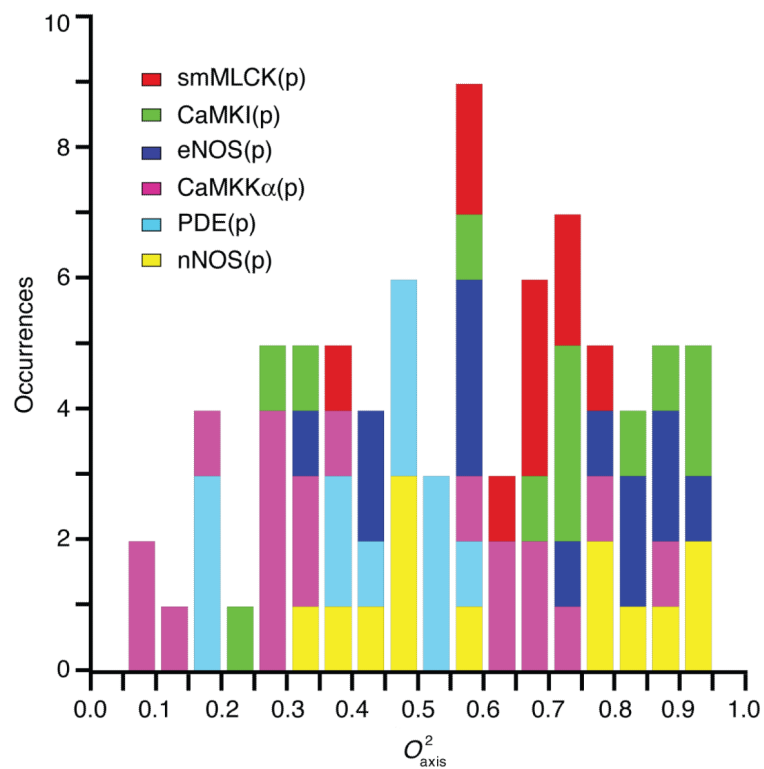


**Figure 1.** Distribution of methyl symmetry axis generalized order parameters ( $O_{axis}^2$ ) for the target domains bound to calcium-saturated wild-type calmodulin (CaM). Determined using deuterium NMR relaxation (see Methods).



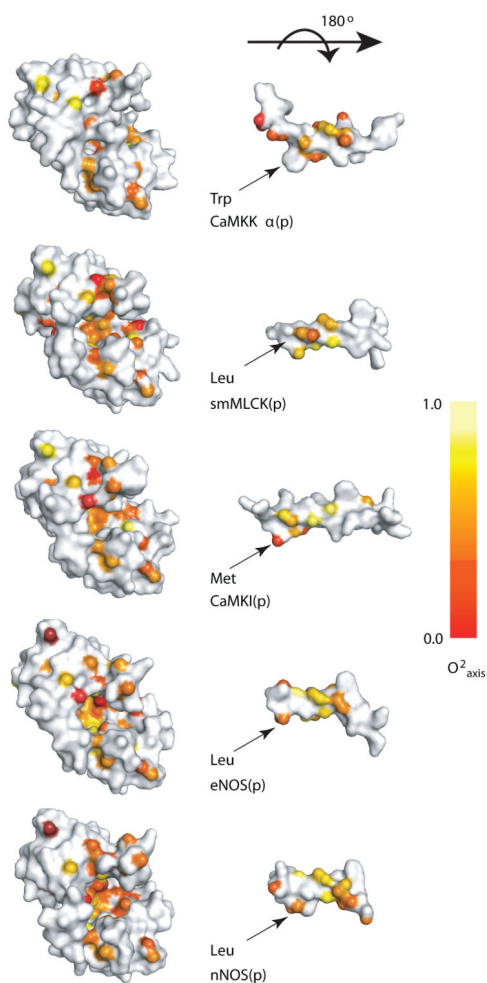


**Figure 2.** Dynamical character of the hydrophobic anchor in the N-terminal domain of CaM. Shown are the heavy atom surface representations of CaM residues 78-144 and the associated target domains. The target domains were flipped 180° and translated to the right to show the binding interface. Circled areas indicate the hydrophobic pockets of CaM. Methyl groups are color coded according to their mobility. The arrows point to the so-called anchor residues. The figure was generated using PyMol<sup>50</sup>.

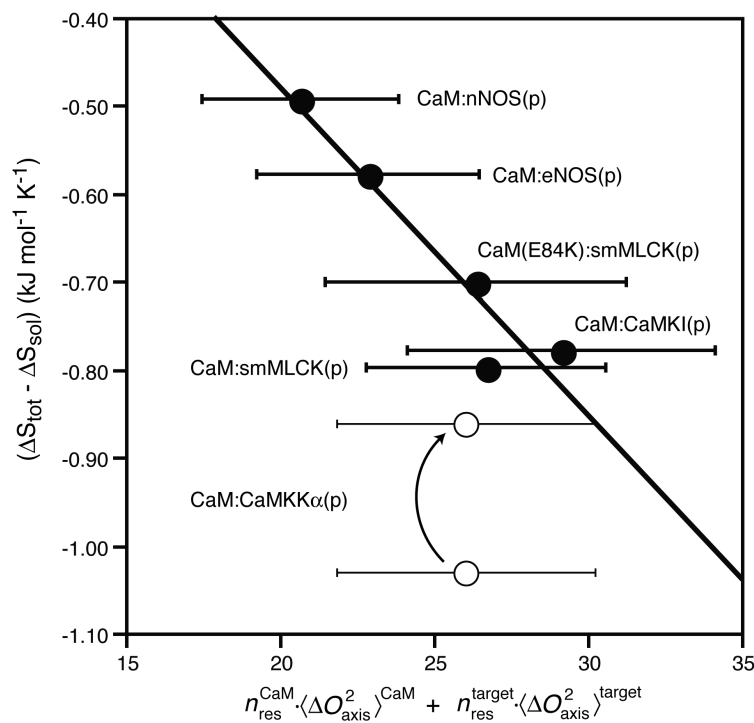


**Figure 3.**

Calibration of the dynamical proxy for protein conformational entropy. Simple considerations lead to the prediction of a quantitative linear relationship between the total binding entropy and the entropy of solvent to the conformational entropy by NMR relaxation parameters derived from methyl bearing amino acids (see Equation 4). The error bars represent the average standard deviation of the difference of the average  $O_{\text{axis}}^2$  parameters between free CaM and the complex with each target (see text). Each  $O_{\text{axis}}^2$  parameter was derived from  $T_1$  and  $T_{1\rho}$  values obtained at two magnetic field strengths. The average dynamics of wild-type and E84K CaM were based on 52 resolved methyl sites. The average dynamics of the six complexes shown were based on 73 to 88 resolved methyl sites (see Supplementary Table 7 for further details). The lower CaM:CaMKKα(p) datum is a clear outlier (Jackknife distance 8.8, all others < 2.3). The upper CaM:CaMKKα(p) point results from a simple correction to the solvent entropy arising from a postulated hydrophobic cluster in the free state of this target domain (see Supplementary Table 5). Excluding the CaM:CaMKKα(p) points results in a linear regression statistic  $R$  of 0.95. This regression line is shown. The slope ( $m = -0.037 \pm 0.007 \text{ kJ K}^{-1} \text{ mol res}^{-1}$ ) allows for empirical calibration of the conversion of changes in side-chain dynamics to a quantitative estimate of changes in conformational entropy. The ordinate intercept is  $0.26 \pm 0.18 \text{ kJ K}^{-1} \text{ mol res}^{-1}$ .

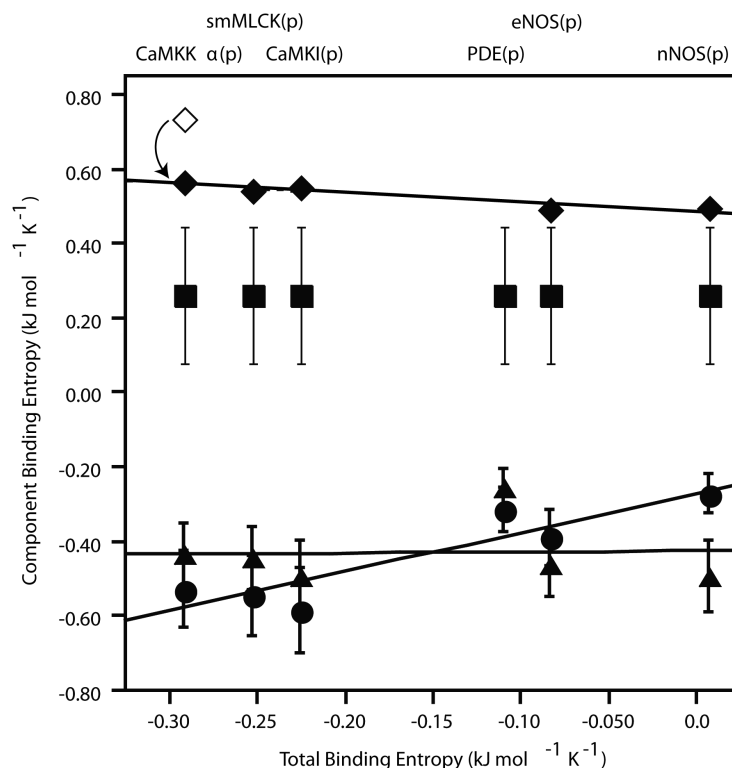


**Figure 4.**

Decomposition of the entropy of binding of target domains to calcium-saturated calmodulin. Based on Equation 4 and the calibration of the dynamical proxy (see Fig. 3) Solid diamonds are the solvent entropies calculated from the changes in accessible surface area and include the correction resulting from the postulated hydrophobic cluster of the free CaMK $\alpha$ (p) target domain (see text and Supplementary Table 5). The uncorrected value for CaMK $\alpha$ (p) is shown as an open diamond. No structure is available for the CaM:PDE(p) complex so the corresponding solvent entropy cannot be calculated. Solid circles and triangles are the contributions to the binding entropy by the conformational entropy of CaM and the target domains, respectively. Solid squares are the contributions to the binding entropy not reflected in the measured dynamics i.e. ( $S_{other} + S_{RT}$ ) (see Equation 4), which is obtained from linear regression (see Fig. 3). Though not required, there are interesting linear correlations between the total binding entropy and its components. There is a significant ( $R = 0.94$ ) but weakly dependent (slope =  $-0.25 \pm 0.04$ ) negative linear correlation between solvent entropy and total binding entropy. In contrast, there is a significant ( $R = 0.91$ ) and relatively strong positive dependence (slope =  $+1.0 \pm 0.2$ ) observed between the change of conformational entropy of CaM and the total binding entropy. The apparent negative correlation between target binding entropy and the total binding entropy is not statistically significant ( $R = 0.045$ ).